lubricants

MDPI

Article

Tribological Evaluation of Lead-Free MoS_2-Based Solid Film Lubricants as Environmentally Friendly Replacements for Aerospace Applications

Parikshit Tonge [1,*], Amit Roy [1,2], Payank Patel [1,2], Charles J. Beall [3] and Pantcho Stoyanov [4,*]

[1] Department of Mechanical, Industrial and Aerospace Engineering, Concordia University, Montreal, QC H3G 1M8, Canada; amit.roy@concordia.ca (A.R.); ppayank13196@gmail.com (P.P.)
[2] Department of Mining and Materials Engineering, McGill University, Montreal, QC H3A 0G4, Canada
[3] Everlube Products, a Business Unit of Curtiss-Wright Corp., 100 Cooper Circle, Peachtree City, GA 30269, USA; Charles_beall@everlubeproducts.com
[4] Department of Chemical and Materials Engineering, Concordia University, Montreal, QC H3G 1M8, Canada
* Correspondence: parikshittonge1995@gmail.com (P.T.); pantcho.stoyanov@concordia.ca (P.S.)

Abstract: Solid lubricants, such as MoS_2 have been widely used in the aerospace industry with the primary purpose of reducing the friction and wear of tribological interfaces. MoS_2 based solid film lubricants are generally doped with other compounds, which can help overcome some of their limitations related to environmental conditions. For instance, compounds like Sb_2O_3 and Pb have been traditionally used to improve the endurance life of these lubricants. However, with the recent zest in transferring to eco-friendly lubricants, there is a strong push to eliminate Pb based compounds. The main purpose of this work is to better understand the influence of Pb based compounds on the tribological behavior of MoS_2 based solid film lubricants as well as to critically evaluate the performance of Pb free lubrication strategies. More specifically, the baseline 'non-green' lubricant was doped with Pb compound and Sb_2O_3 and the Pb compound in the 'Green' alternative lubricant was replaced by more Sb_2O_3. The wear test was done using a ball-on-disk tribometer for specific loads and for 5000 cycles. Ex-situ analysis was conducted using Scanning Electron Microscope (SEM), Atomic Force Microscopy (AFM), and micro-Raman to capture the interfacial processes of these lubricants at different loads. Overall, the non-green lubricant performed better in terms of the tribological behavior (i.e., lower friction and wear), which was attributed to the formation of a dense MoS_2-based tribo-/transfer-film with the basal planes oriented in the parallel direction to the sliding. The finding on the interfacial phenomena provided critical insights into the development of novel green alternatives that may have the ability to replace Pb based compounds in the future for a sustainable environment.

Keywords: solid lubricant; non-green; tribological behavior; interfacial processes; transfer-film

check for updates

Citation: Tonge, P.; Roy, A.; Patel, P.; Beall, C.J.; Stoyanov, P. Tribological Evaluation of Lead-Free MoS_2-Based Solid Film Lubricants as Environmentally Friendly Replacements for Aerospace Applications. *Lubricants* **2022**, *10*, 7. https://doi.org/10.3390/lubricants10010007

Received: 2 December 2021
Accepted: 1 January 2022
Published: 6 January 2022

1. Introduction

Solid lubricants are commonly employed in tribological interfaces with the purpose to reduce friction and increase the wear resistance of the component. While there are many commercially available solid lubricants (e.g., Graphite, MoS_2, WS_2, PTFE, etc. [1]), MoS_2 –based solid lubricants are most frequently used in extreme environments, such as gas turbine engines [2], due to their favorable tribological behavior (e.g., low friction and low wear). MoS_2 has a layered structure that consists of one atom of Mo which is sandwiched between 2 atoms of S. There exists a strong covalent bond between Mo–S atoms and a weak Van Der Waals attraction between the layers of the atoms [3,4]. The main drawback of using MoS_2 is that its tribological behavior is very sensitive to environmental conditions. While pure MoS_2 performs well in vacuum conditions, it can exhibit higher friction and premature failure when operating in humid/ambient conditions, which is sometimes attributed to the formation of MoO_3 [5,6]. To overcome some of these challenges, MoS_2 is usually doped with metals/composites, such as Au, Ti, Ni, Ag, PbO, Sb_2O_3, WS_2, WSe_2, etc. [1,3,4,7–9] These compounds make the composite coating more reliable and also improves the tribological performance in the ambient conditions. In particular, lead based MoS_2 lubricants have traditionally been used in the aerospace community due to their favorable stability. Pb also has some exceptional features, such as softness, low melting point, high ductility and resistance to corrosion which makes the usage of Pb very critical in the Aerospace Industry [10]. However, due to its toxic nature and its adverse effects on the environment, the usage of Pb has been reduced and many green alternatives have been proposed [10–12].

Wahl et al. [13] showed that MoS_2 doped with a small amount of PbO results in relatively high wear resistance and lower frictional coefficients than pure MoS_2 [14–16]. The sliding induced crystallinity has been observed in Pb based MoS_2 lubricants through Raman Spectroscopy [13,15]. More specifically, at the sliding interface, the initial amorphous MoS_2 coating was converted into crystalline MoS_2 due to the mechanical stresses [13]. However, with crystalline MoS_2, there is a possibility of high wear during the initial stages of sliding which may cause the fracture of crystallites in the microstructure [14,17]. This behavior was not observed for the amorphous Pb-doped MoS_2 films, which could possibly be explained by the fact that the Pb-doped MoS_2 lubricants are less sensitive to delamination [14].

While Pb basedMoS_2 lubricants provide better tribological performance over other solid lubricants, there is a strong desire to replace Pb with 'green alternatives' due to health and environmental concerns. One compound that is commonly doped with MoS_2 solid lubricants is Sb_2O_3 [6]. While Sb_2O_3 is not a self-lubricating compound, it has shown to be an effective dopant to MoS_2 in reducing friction and wear. Three main advantages of adding Sb_2O_3 to the composite have been identified in the literature as follows: (i) Sb_2O_3 reduces the intercolumnar porosity and thus, increases density and increases hardness, (ii) it serves as an oxidation barrier and also (iii) it inhibits the crack growth by making the film harder [1,8,18–20].

The main purpose of this study is to compare the tribological behavior of Pb based MoS_2 dry film lubricant (non-green lubricant) to Pb free MoS_2 based dry film lubricant (green lubricant) under a wide range of contact conditions. While both, the green and non-green solid film lubricants are doped with Sb_2O_3, the lubrications strategy for the 'green' alternative was to replace the Pb content with an additional amount of Sb_2O_3. The solid film lubricants were evaluated in terms of their tribological behavior at a wide range of contact stresses, mimicking conditions observed in gas turbine engines. This study has employed some of the characterization techniques, such as SEM, AFM and micro-Raman to provide a better understanding of the interfacial phenomena and the chemical nature of the coatings. The observations from the EDS analysis and the mapping were correlated to the adhesive forces measured using atomic force microscopy. In addition, the tribofilms of the lubricants were investigated in detail by means of Raman spectroscopy in terms of their composition and structure.

2. Materials & Methods

In this study, two solid film lubricants are characterized in terms of their tribological behavior. The two solid film lubricants are Everlube 620C (green lubricant) and Lube-Lok 5306 (non-green lubricant). Everlube 620C is composed of MoS_2, Sb_2O_3 (5–10 wt.%), and organic compounds as binders. Lube-Lok 5306 has MoS_2, Sb_2O_3 (<10 wt.%), lead phosphite (<5 wt.%) and organic compounds as binders. More details on the composition of the solid film lubricants can be found elsewhere [21]. The main difference between the 'green' and 'non-green' lubricant is that the lead phosphite present in the 'non-green' version is replaced with an additional amount of Sb_2O_3 in the 'green' lubricant. The MoS_2-based solid film lubricants were deposited onto 304L stainless steel substrates. The solid film lubricants were deposited using the dip spin process. More details on the process can be found elsewhere [22]. Briefly, prior to the deposition, the stainless-steel substrates were surface polished using the Struers Tegramin polishing and grinding equipment. The surface roughness of the polished sample was measured to be 0.09 microns. Subsequently, grit-blasting was done as a pre-treatment process (i.e., 220 Al_2O_3 grit size was used for grit-blasting). The thickness of the lubricants was in the range of 11-13 microns.

Tribology testing was performed by means of a ball-on-disk linear tribometer (Anton-paar TRB^3 tribometer) using five different loads (i.e., 1 N, 5 N, 8 N, 10 N, 13 N) for 5000 cycles. The sliding speed was set at 3.1 cm/s, which corresponds to a frequency of 1 Hz. The sliding tests were performed for a stroke length of 10 mm. The testing was conducted at room temperature (25–28 °C) and the Relative Humidity was controlled between 15% and 20% by the use of desiccants. The counterface used for the testing was Al_2O_3 with a diameter of 6.35 mm. After the sliding tests, the wear depths were measured using LEXT Confocal Laser Microscopy and also the optical images of the counterfaces were obtained using the Confocal Laser Microscope. The schematic diagram of the tribometer is adapted from one of the author's previously reported works [23].

Coating characterization was performed by means of Hitachi High Technologies America, Inc., USA Scanning Electron Microscope (SEM), Energy Dispersive Spectroscopy (EDS) (Pentafet Link, INCA X-sight, Oxford instruments, UK) and Anton–paar Tosca 400 Atomic Force Microscopy (AFM), Switzerland. The SEM was used to obtain the high-resolution images of the wear tracks and the counterfaces and also to study the topography of the images. The EDS analysis was performed on the worn (5 N and 10 N) and unworn surfaces as well as on counterfaces in order to obtain the elemental composition. Subsequently, the AFM was used to obtain the pull-off force (adhesion force) and also to study the resistance to plastic deformation of the coatings. A total of 10 tests (five on worn surface and five on unworn surface) were performed per sample under the contact mode. An FDC curve is generated due to the deflection in the cantilever tip which helps in determining the maximum adhesion force. A typical Force-Displacement curve is shown in Figure 1 [24,25]. Finally, Micro-Raman spectroscopy was performed on a 10 N worn surface using CNI MGL-U-532 equipped with High Stability DPSS Laser (532 nm), Chinato understand the crystallinity on the worn surfaces.

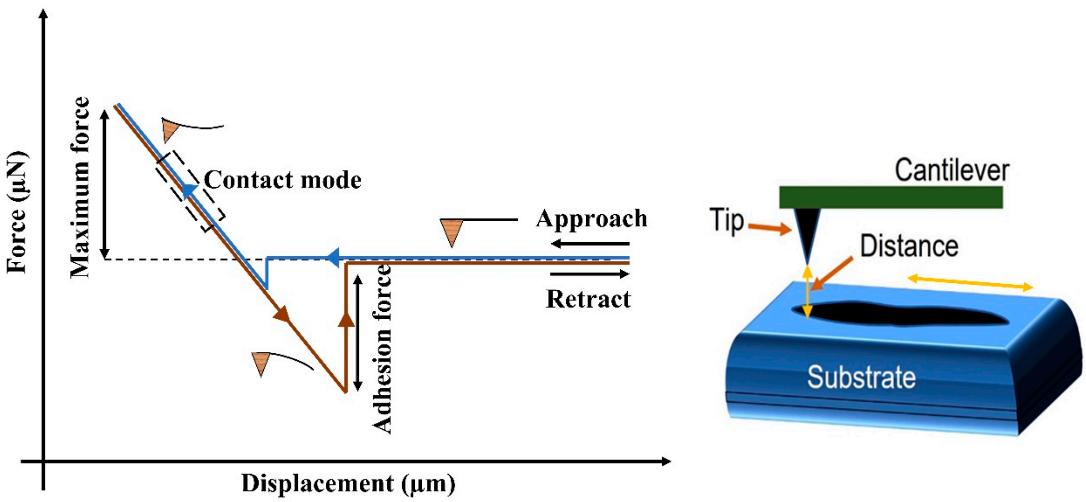

Figure 1. Determining adhesion force using Force—Displacement curve [24].

3. Results

3.1. Friction Behavior

Figure 2 shows the friction behavior vs. the number of cycles for the green and non-green solid film lubricants. For both lubricants, the coefficient of friction decreased with increasing the normal load. A break-in phases of up to approximately 200 cycles is observed for all conditions. Subsequently, to the break-in phase, the friction coefficient remains relatively steady for the remainder of the test (i.e., steady state regime) with all normal loads except for 13 N on green lubricant. As shown in Figure 2a, with a 13 N load, the green lubricant had worn out resulting in high friction. It should be noted that for the first test with a 13 N load, the lubricant started to wear out at around 3000 cycles, however, during the repeat, the lubricant remained intact and showed a steady state coefficient of friction of 0.09.

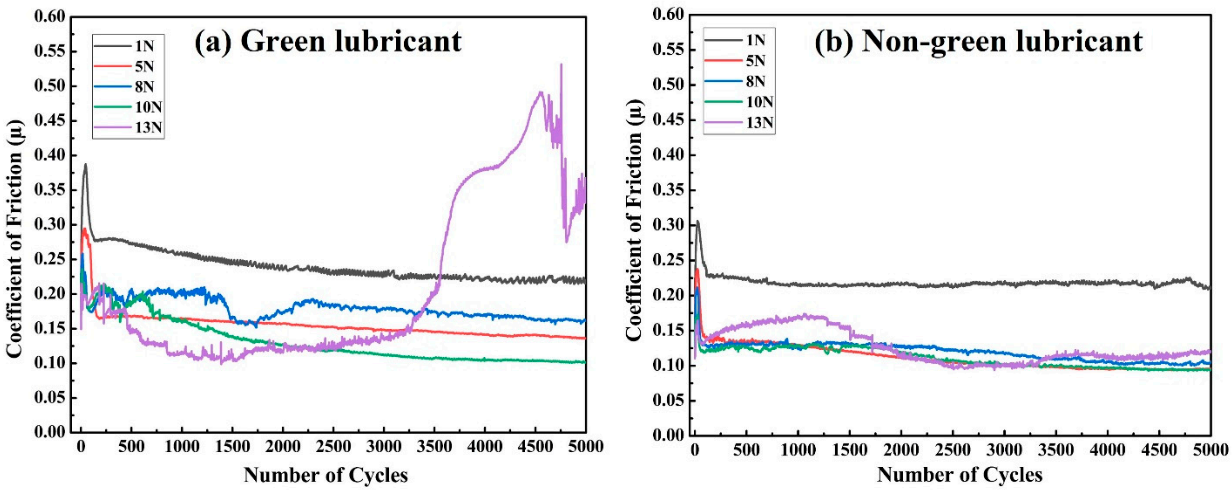

Figure 2. Friction coefficient vs. Number of Cycles with various normal loads for (**a**) Green lubricant and (**b**) Non-green lubricant.

Figure 3 shows the average steady state friction coefficient vs. the Hertzian contact pressures. The corresponding Hertzian contact stresses are calculated for the above-mentioned five different loads which range in between 0.68–1.62 GPa. More details on the calculation of the Hertzian contact stress can be found elsewhere [26]

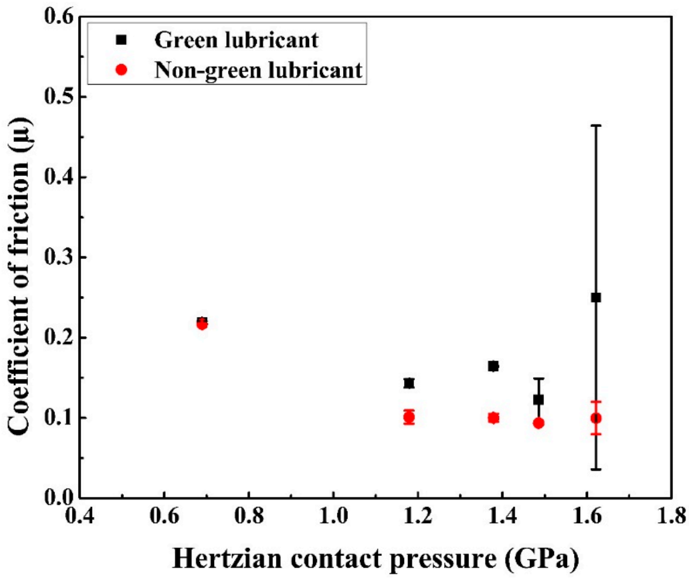

Figure 3. Friction coefficient vs. Hertzian Contact Pressure.

Overall, the non-green lubricant (Lube-Lok 5306) showed lower friction values for different contact pressures. The green lubricant showed a large deviation in the friction values with the13 N load, which can be explained by the premature failure of the lubricant at about 3000 cycles, as shown in Figure 2a. This behavior was an indication that the non-green lubricant has a better load carrying capacity compared to the green lubricant. Thus, the inclusion of Pb seems to have an evident impact on the coefficient of friction results.

Figure 4 shows the graph between the friction force and the normal force. A linear fit was performed in correspondence to F~L^m. The slope from the linear fit corresponds to m, which showed a value of 0.83 for the green lubricant and 0.69 for the non-green lubricant. The m value of 0.69 for the green lubricant is much closer to F~$L^{2/3}$ which corresponds to Hertzian elastic contact mode [4,27].

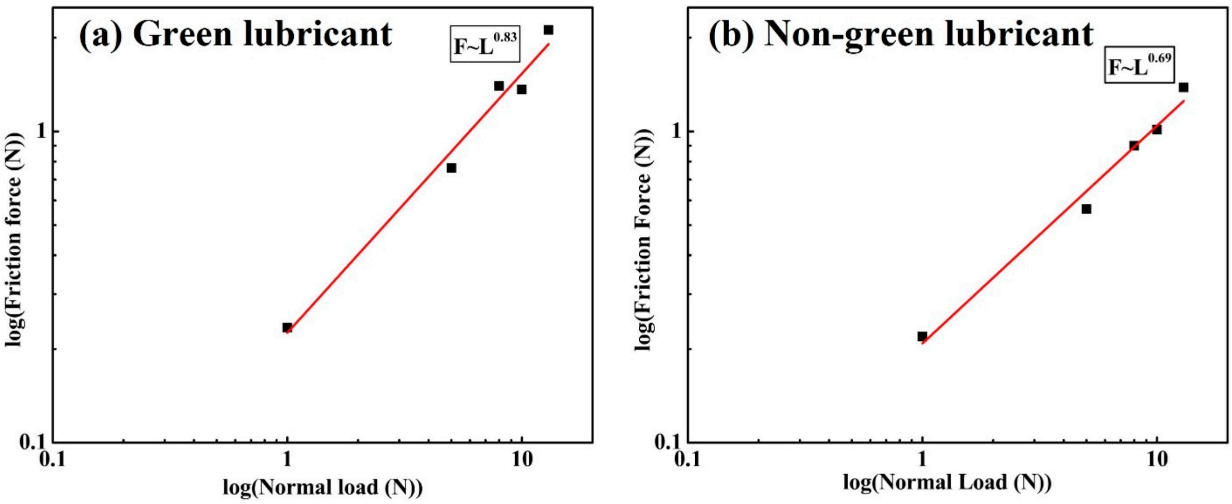

Figure 4. Friction Force vs. Normal Load for (**a**) Green lubricant and (**b**) non-green lubricant.

3.2. Wear Behavior

Figure 5 shows the wear profiles of both lubricants for the various normal loads used throughout the testing. The behavior was quite different from the behavior of the coefficient of friction. Overall, the wear for both lubricants increases with increasing normal load. However, the wear depth for all conditions is lower for the non-green lubricant when compared with green lubricant. In particular, when using normal loads above 5 N, the wear of the green lubricant is evidently higher than the non-green lubricant.

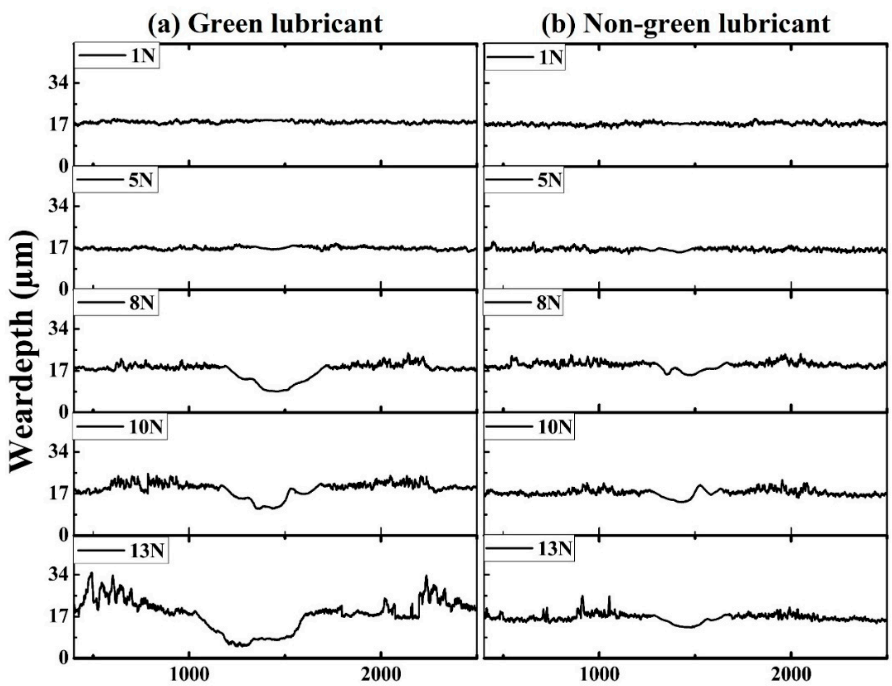

Figure 5. Wear depths of (**a**) green lubricant (**b**) non-green lubricant.

3.3. Ex Situ Analysis

Figure 6 shows the worn surface morphology of green lubricant and non-green lubricant at both 5 N and 10 N loads. In all conditions, the worn surfaces appear to have formed smooth tribofilms. However, the images of the green lubricant revealed the formation of cracks for 10 N, which were less evident with the non-green lubricant. Figure 6c,d shows the wear tracks of green and non-green lubricant at 5 N load, which seems to be less uniform when compared to the tests with the higher normal loads. The tribofilms on the worn surface are shown on the magnified SEM images at both the normal loads.

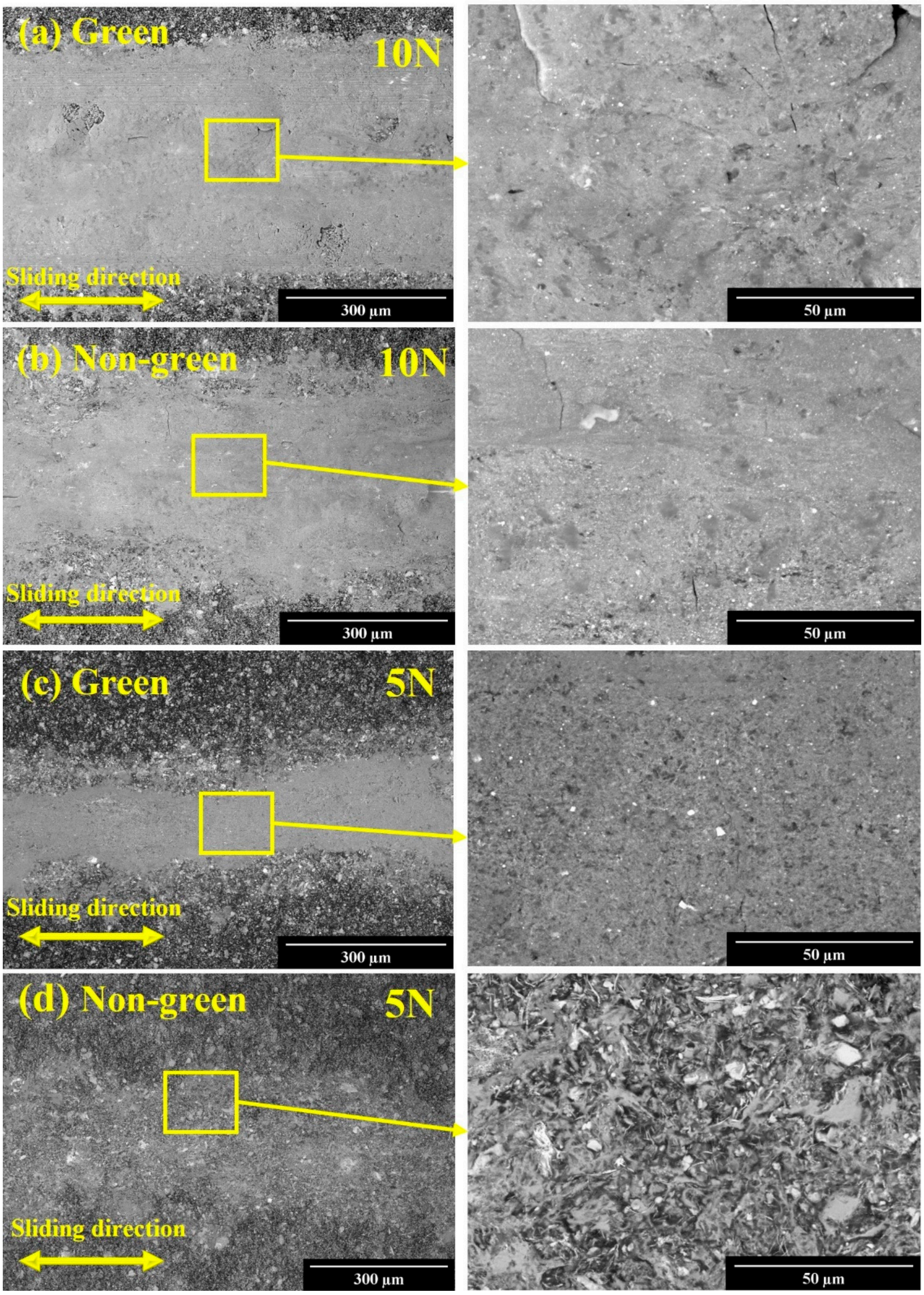

Figure 6. Wear scars of (**a**) green lubricant at 10 N (**b**) non-green lubricant at 10 N (**c**) green lubricant at 5 N (**d**) non-green lubricant at 5 N.

Figure 7 shows the elemental maps of the wear tracks for both lubricants. The EDX analysis and the elemental maps suggested the presence of Mo, S, Sb, O as the main components in green lubricant. Similarly, the same elements were observed in non-green lubricant with the addition of Pb. The atomic percentages of the elements in green lubricant are Mo (5.89 ± 0.93), S (9.54 ± 1.46), Sb (1.86 ± 0.79), O (13.50 ± 3.55) and Fe (2.03 ± 2.95). The atomic percentages of the elements in non-green lubricant are Mo (7.86 ± 2.66), S (12.59 ± 4.45), Sb (1.25 ± 0.72), O (12.06 ± 6.24), Pb (0.25 ± 0.23) and Fe (0.27 ± 0.05). In addition, the atomic percentages and EDX maps in Figure 7a showed the traces of Fe content for green lubricant, which indicated that parts of the solid lubricant have been worn out. This correlates well with the observation of the coefficient of friction for the 13 N load test, where the coating has worn out.

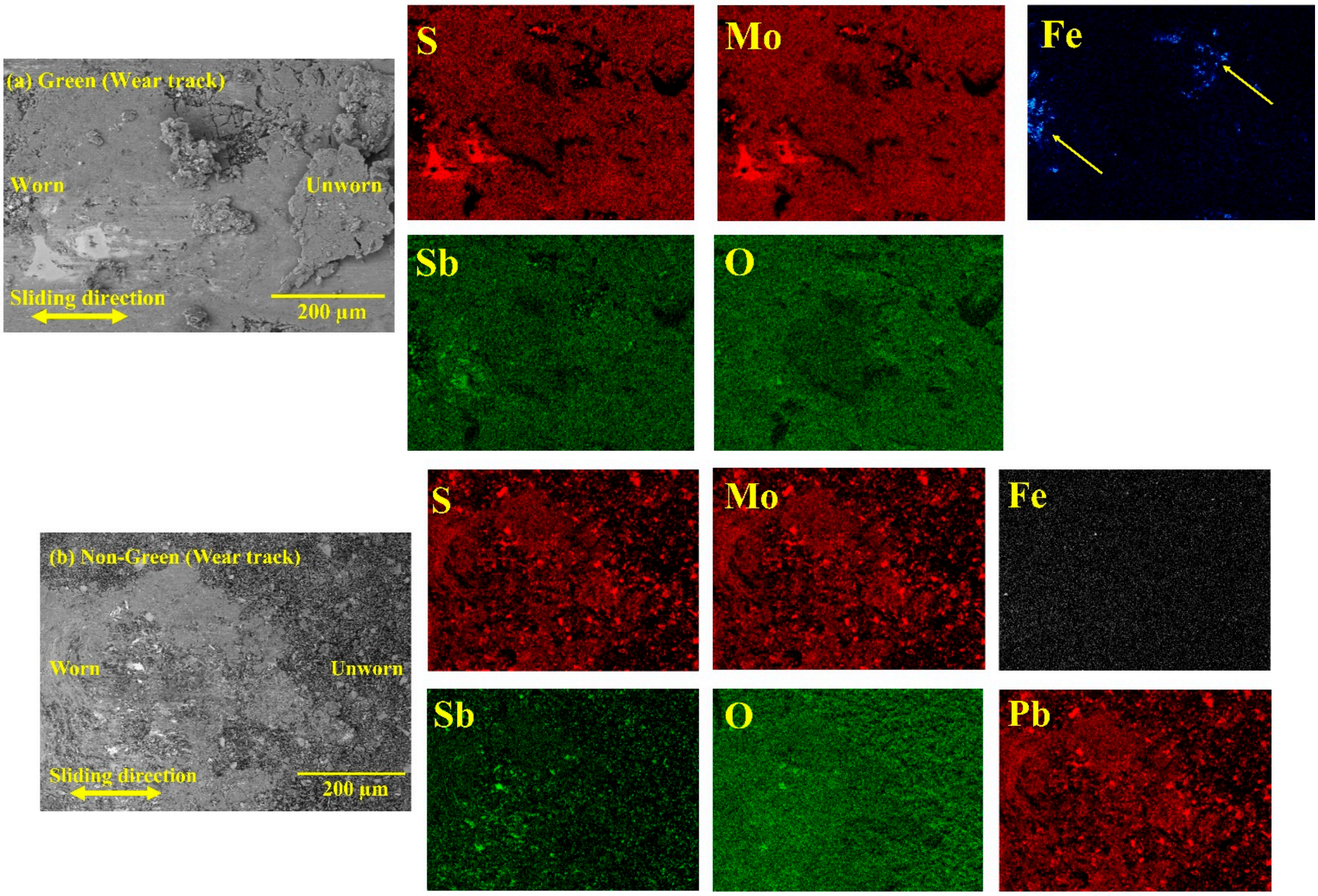

Figure 7. (**a**). EDS mapping of green lubricant worn surface at 10 N load. (**b**). EDS mapping of non-green lubricant worn surface at 10 N load.

Figure 8 shows the Raman spectroscopy on both the coatings for the worn and unworn surfaces. The peaks at Raman shift approximately 380 cm^{-1} and 400 cm^{-1} are clearly visible from Figure 8 which corresponds to crystalline MoS_2 [4,5,9]. For unworn surfaces of both, the green and non-green lubricants, (Figure 8b,d), the intensity of the peaks corresponding to MoS_2 was similar for both lubricants and relatively low, which could be due to the influence of the additional elements in the lubricant in the as deposited condition. Figure 8a,c shows the Raman spectra of the corresponding worn surfaces, indicating visible peaks associated with MoS_2. The worn surface of the non-green lubricant shows a higher intensity peak associated with MoS_2 compared to green lubricant, which could indicate that the tribofilm formed with non-green lubricant was MoS_2 rich and more uniform compared to the green lubricant. In addition, this could be due to the basal planes of the MoS_2 oriented parallel to the sliding direction [4].

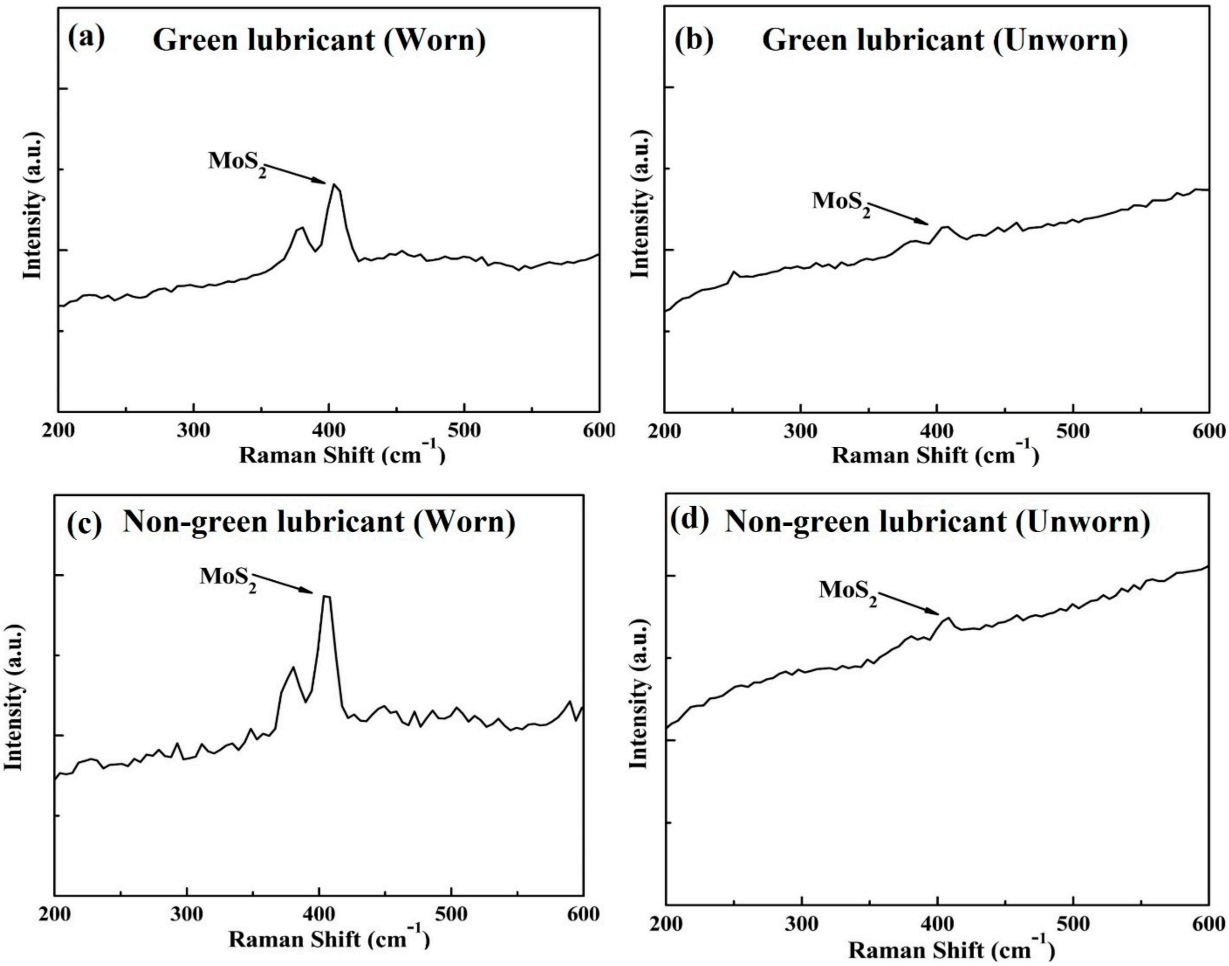

Figure 8. Film characterization using Raman Spectra for (**a**) green lubricant (worn), (**b**) green lubricant (unworn), (**c**) non-green lubricant (Worn) and (**d**) non-green lubricant (unworn).

Figure 9 represents the pull-off force measurements obtained from the AFM testing. The adhesion (i.e., pull-off) force for both the lubricants was measured by AFM using the Force-Spectroscopy method. The adhesive force is nearly identical for the unworn surfaces of both the lubricants, however, the adhesive force on the worn surface of the green lubricant is evidently higher than the worn surface of the non-green lubricant. In the ambient conditions, the adhesion force typically consists of Van der Waals force, electrostatic force and capillary force [28]. Thus, the observations from the AFM correlate well with the Raman spectra, indicating that there is a higher amount of MoS_2 present on the worn surface of non-green lubricant with the basal planes oriented in the parallel direction to the sliding.

Figure 10 represents the indentation depth (i.e., inversely proportional to the nano-hardness) of both the lubricants on both the worn and unworn surfaces. The wear depth on the worn surfaces was higher for the green lubricant when compared with non-green lubricant, which illustrates that the tribofilm on the non-green lubricant is harder compared to the one on the green lubricant. Hardness is also increased with increasing density and reduced porosity of the film, which ultimately can help in reducing friction and wear. This is similar to the influence of the hardness of the bulk lubricant on friction and wear [1,6].

Figure 11 represents the SEM images of the counterfaces for green lubricant and non-green lubricant for 10 N load. When compared with green lubricant, the non-green lubricant has a more uniform transfer film, which can result in lower friction and wear. As shown in Figure 11, at 10 N load, the amount of debris particles visible is similar for the solid lubricants. However, at 5 N load, a significantly higher amount of loose debris particles can be seen with green lubricant.

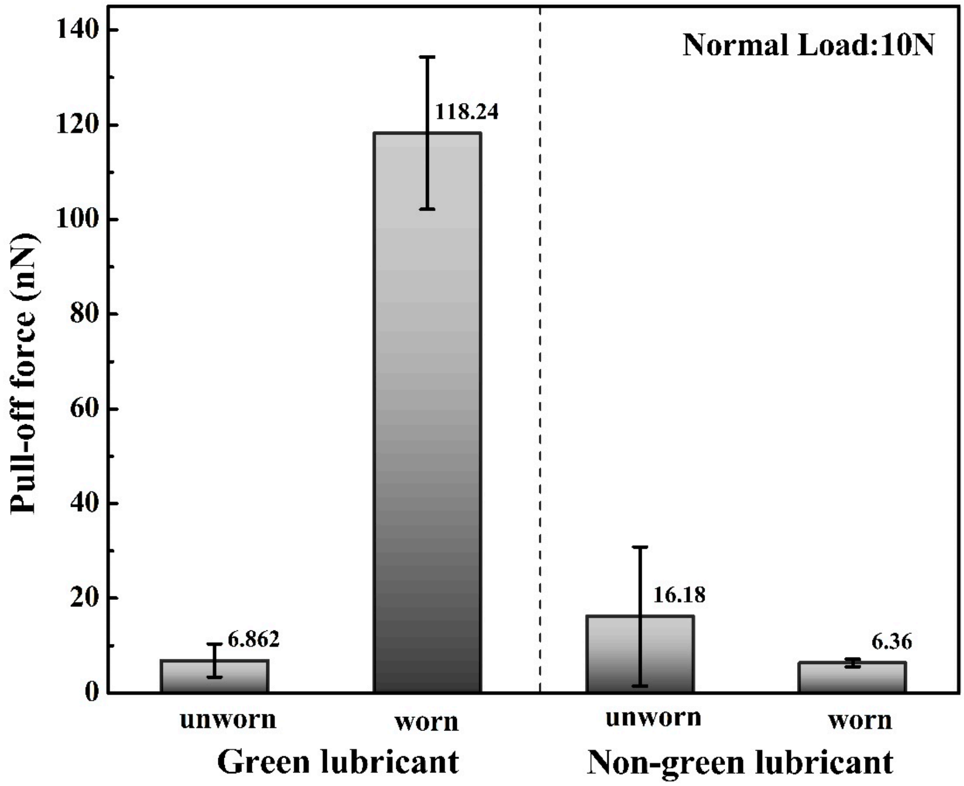

Figure 9. Pull-off force measurement using AFM Spectroscopy at 10 N load.

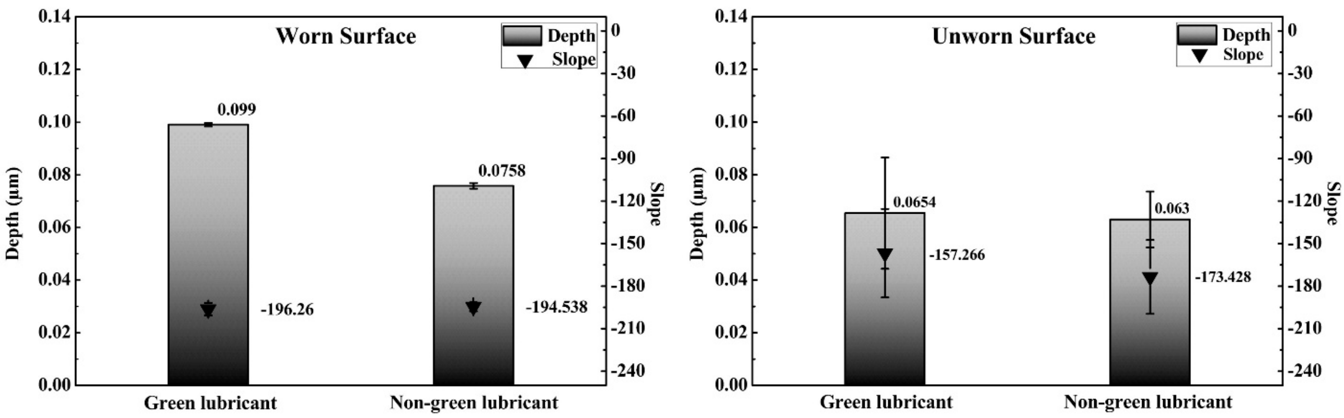

Figure 10. Estimation of hardness of lubricants using AFM Spectroscopy on (**a**) Worn Surface and (**b**) Unworn Surface.

Figure 12 shows the elemental maps of the counterfaces for both, the green lubricant and non-green lubricant. The EDX analysis shows the presence of Mo, S, Al, Sb and O as the main components in green lubricant and the same elements with the addition of Pb in non-green lubricant. As per EDX analysis, a higher atomic percentage of Sb is observed in green lubricant (3.46 $\pm$ 0.75) rather than in non-green lubricant (1.79 $\pm$ 0.75), which indicates a higher amount of three-body abrasion with green lubricant.

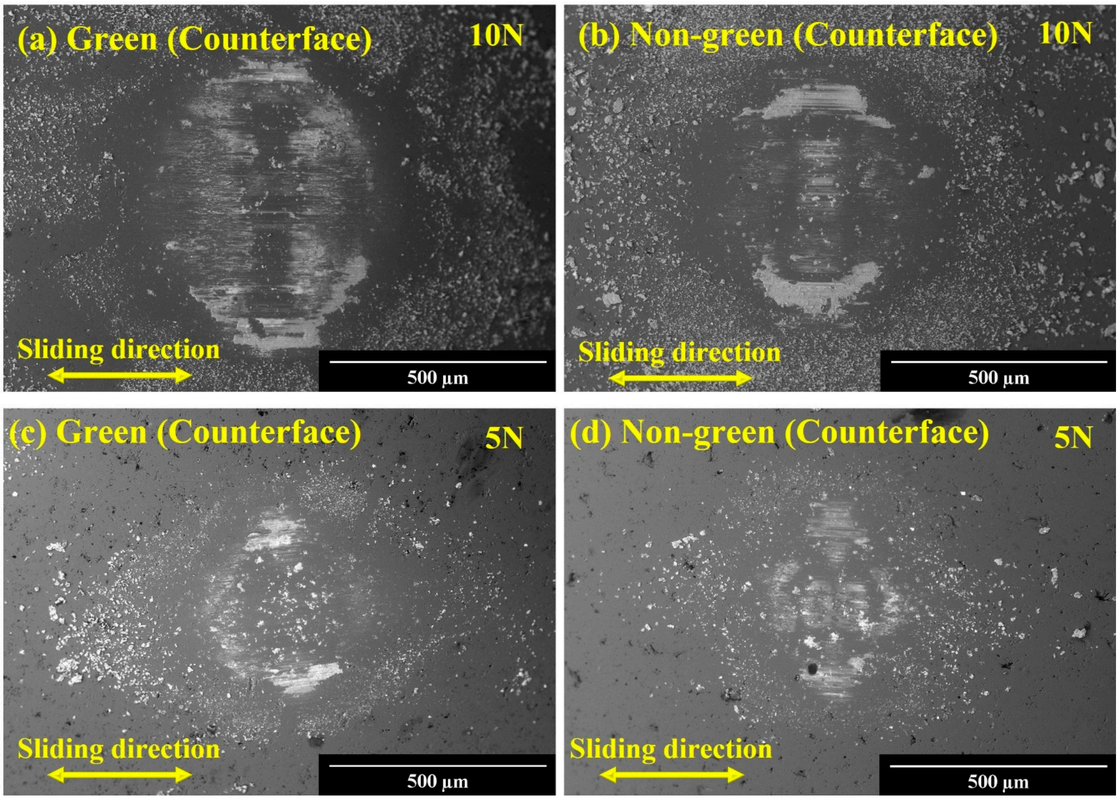

Figure 11. SEM image of counterface for (**a**) green lubricant at 10 N (**b**) non-green lubricant at 10 N (**c**) green lubricant at 5 N (**d**) non-green lubricant at 5 N.

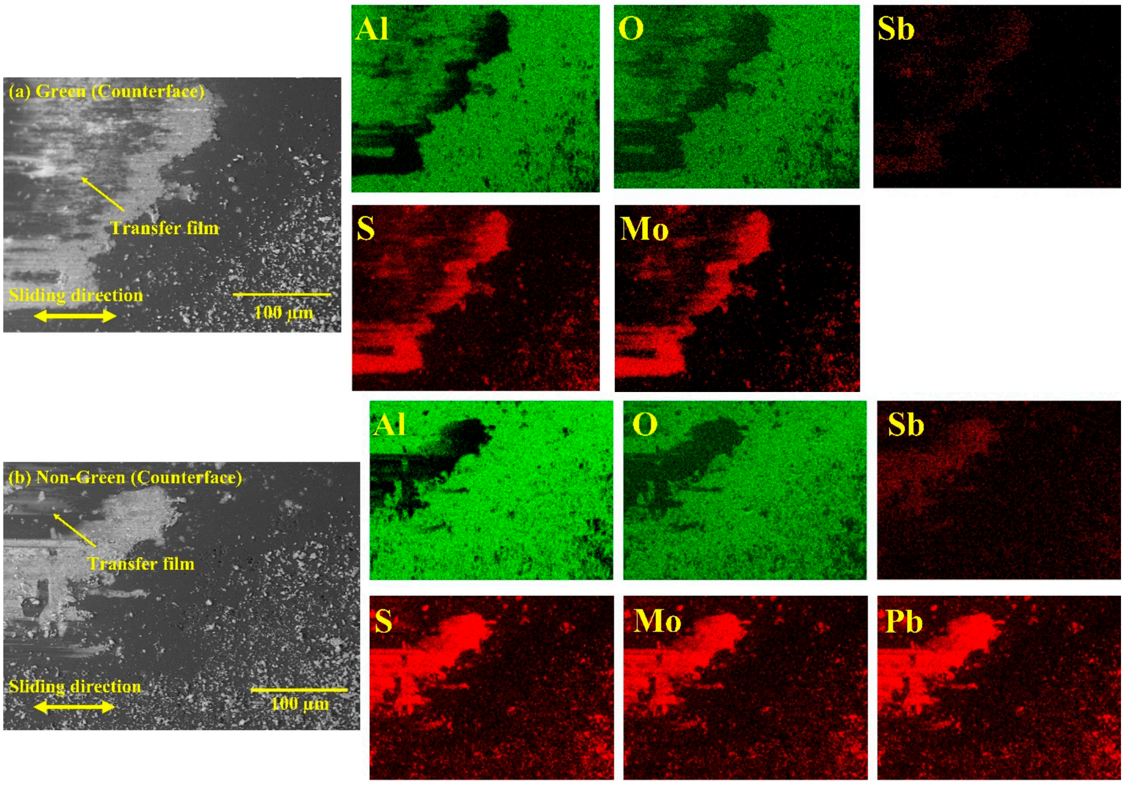

Figure 12. (**a**). EDS mapping of green lubricant counterface at 10 N load. (**b**). EDS mapping of non-green lubricant counterface at 10 N load.

4. Discussion

In order to fully capture the tribological behavior of green lubricant and non-green lubricant, it is important to first understand the effect of dopants on the performance of MoS_2. In general, the addition of dopants to MoS_2 imparts specific physical and chemical properties which help in improving the tribological performance of the overall coating. According to literature, the addition of Sb_2O_3 helps the coating in preventing crack growth [8]. In addition, Sb_2O_3 also helps in reducing the intercolumnar porosity and increases the oxidation resistance [8,19,20]. Similarly, the addition of Pb as a dopant also improves the oxidation resistance, however, also facilitates the formation of basally oriented MoS_2 crystallites, as well as increases the hardness and possibly the elastic modulus of the MoS_2 film [13,15,29,30].

The observations from the tribological testing performed in this study showed that non-green lubricant overall performs better in both, reducing the friction coefficients and the wear depth when compared to the green lubricant. The friction and wear behavior correlated well with the observations from the ex-situ analysis. For instance, the MoS_2 peaks obtained with the Raman spectroscopy (Figure 8) were higher in intensity on the worn surface of the non-green lubricant compared to the green lubricant one. This observation indicated that the tribofilm formed on the 'non-green' lubricant contains a higher amount of MoS_2, which is potentially more crystalline in nature [4]. As pointed out above, the addition of Pb to MoS_2 increases the hardness, and therefore, can facilitate the formation of a thin tribofilm and transfer film with basally oriented MoS_2 crystallites. Previous studies have shown that when the basal planes of the MoS_2 are oriented parallel to the substrate, the films showed lower friction coefficient, improved oxidation resistance and increased wear life [1,8,31]. Thus, for the test conditions in this study, the improved wear resistance and reduced friction with the non-green lubricant can be attributed to the presence of a small amount of Pb, which helped with the formation of a more desirable tribofilm. Consequently, this results in a Hertzian elastic sliding mode with the non-green lubricant following $F{\sim}L^{2/3}$ as shown in Figure 4. In addition, the ex-situ analysis by means of AFM showed higher adhesive force (pull-off) present on the worn surface for the green lubricant compared to the non-green one (Figure 9). This is in line with the observations from the Raman analysis, where the tribofilm generated on the non-green lubricant contains a higher amount of MoS_2 with the basal planes oriented in the parallel direction to the sliding. The lower adhesive force on the surface with the basal planes oriented parallel to the sliding direction can be explained by the fact that the basal planes have lower surface energies compared to the edge planes in the MoS_2 [32]. In addition, the tribofilm generated on the non-green sample may be denser and thus, have a higher hardness, which can result in reduced surface adhesion [33].

Similarly, to the tribofilm, the transfer film generated with the non-green lubricant appears to be more uniform within the contact area. This can possibly be explained by the higher amount of three-body abrasive wear with green lubricant, which is attributed to the higher amount of Sb_2O_3. The Sb_2O_3 can act as abrasive particles within the contact and make it more difficult for transfer film formation.

Figure 13a shows the wear mechanisms for non-green lubricants and Figure 13b shows the wear mechanism for green lubricants. For both lubricants, during the initial sliding, debris particles are generated and get attached to the counterface (as shown in Figure 11). As per Singer et al. [34], the wear debris can be the compacted wear debris or the loose powdery wear debris. This compacted wear debris during the further sliding helps in the formation of the transfer films. Loose debris particles are often seen in sliding contacts and these debris particles can be either generated during sliding or from reacting with the surrounding environment [35,36]. These particles can influence the friction and wear depending on the coating thickness and the hardness of the coating. The compacted wear particles that are trapped are free to slide and thus sometimes form the transfer films [34]. In the case of the 'non-green' lubricant, upon further sliding, MoS_2 rich tribofilm and transfer film are formed resulting in lower friction and wear. For the green dry film lubricant, the formation of a dense and uniform tribo-/transfer-film is hindered by the higher amount of Sb_2O_3 particles present in the lubricant. Consequently, the insufficient tribo-/transfer-film formation results in higher friction and wear.

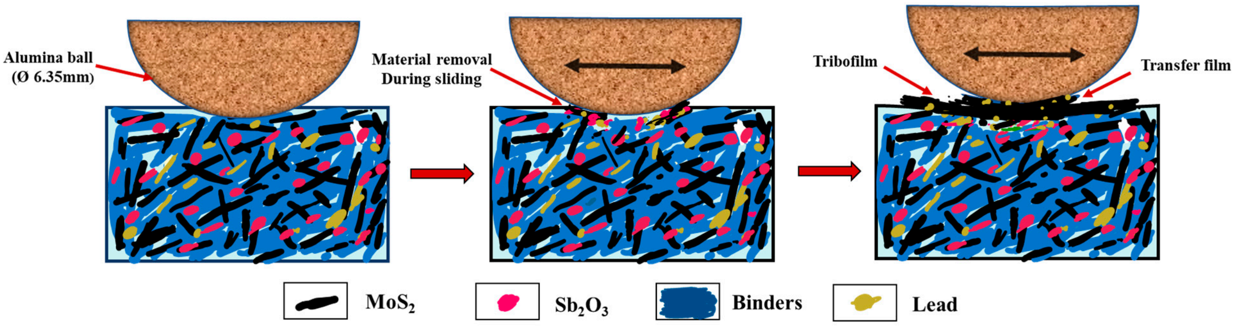

(**a**)

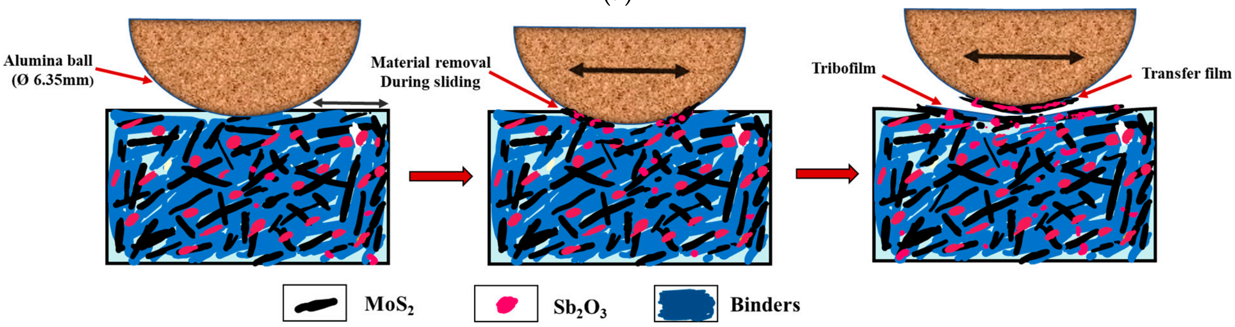

(**b**)

Figure 13. (**a**). Wear mechanism for non-green lubricant (Less amount of loose debris particles are observed which helped in the formation of uniform and dense transfer film). (**b**). Wear mechanism for green lubricant (Higher amount of loose Sb_2O_3 particles are observed which restrict the sufficient amount of tribofilm and transfer film formation).

5. Conclusions

In the present study, 'Non-green' and 'Green' MoS_2 based solid film lubricants were deposited using the dip spin process, and the tribological behavior was evaluated under the ambient conditions. The following conclusions have been made:

- The tribological performance of green and non-green solid lubricants was investigated at various loads (1 N to 13 N) in dry sliding conditions against alumina counterface.
- The non-green solid film lubricant showed lower coefficients of friction and wear as well as improved load carrying capacity when compared to the green lubricant.
- The presence of Pb during the sliding motion helps the MoS_2 crystallites to orient themselves in the parallel direction to the substrate
- The presence of the Pb has increased the hardness and potentially increased the density.
- The green lubricant resulted in more generation of loose debris particles (i.e., antimony trioxide) which made it difficult to form a thin and uniform transfer film.

Although, the Pb based MoS_2 solid lubricant in this study performed overall better in terms of the tribological behavior (i.e., lower friction and wear), the finding of the interfacial phenomena provided critical insights into the development of novel green alternatives that may have the ability to replace Pb based compounds in the future for sustainable environment.

Author Contributions: Original manuscript draft writing, experimental and data analysis, P.T.; Data analysis and critical review, A.R.; Data analysis and critical review P.P.; Experimental and critical review, C.J.B.; Supervision, conceptualization, modification in revised version, critical review and research funding P.S. All authors have read and agreed to the published version of the manuscript.

Funding: There was no external funding involved in this project.

Data Availability Statement: The data presented in this study are available on request from the corresponding author.

Acknowledgments: Authors would like to acknowledge Everlube Products for providing the deposited samples. The authors would like to thank Fadhel Ben Ettouil for his assistance during the experimental work.

Conflicts of Interest: The authors declare no conflict of interest.

References

1. Scharf, T.W.; Kotula, P.G.; Prasad, S.V. Friction and wear mechanisms in MoS2/Sb2O3/Au nanocomposite coatings. *Acta Mater.* **2010**, *58*, 4100–4109. [CrossRef]
2. Aouadi, S.M.; Paudel, Y.; Luster, B.; Stadler, S.; Kohli, P.; Muratore, C.; Hager, C.; Voevodin, A.A. Adaptive Mo 2N/MoS 2/Ag tribological nanocomposite coatings for aerospace applications. *Tribol. Lett.* **2008**, *29*, 95–103. [CrossRef]
3. Spalvins, T. Frictional and morphological properties of Au-MoS2 films sputtered from a compact target. *Thin Solid Films* **1984**, *118*, 375–384. [CrossRef]
4. Stoyanov, P. Microtribological Performance of Metal-Doped MoS2 Coatings. Ph.D. Thesis, Mcgill University, Montréal, QC, Canada, 2011.
5. Paradecka, A.; Lukaszkowicz, K.; Sondor, J.; Pancielejko, M. Structure and tribological properties of MoS2 low friction thin films. *ITM Web Conf.* **2017**, *15*, 06008. [CrossRef]
6. Vazirisereshk, M.R.; Martini, A.; Strubbe, D.A.; Baykara, M.Z. Solid Lubrication with MoS2: A Review. *Lubricants* **2019**, *7*, 57. [CrossRef]
7. Hu, J.J.; Bultman, J.E.; Zabinski, J.S. Microstructure and lubrication mechanism of multilayered MoS2/Sb2O3 thin films. *Tribol. Lett.* **2006**, *21*, 169–174. [CrossRef]
8. Singh, H.; Mutyala, K.C.; Evans, R.D.; Doll, G.L. An investigation of material and tribological properties of Sb2O3/Au-doped MoS2 solid lubricant films under sliding and rolling contact in different environments. *Surf. Coat. Technol.* **2015**, *284*, 281–289. [CrossRef]
9. Bickford, J. *Handbook of Bolts and Bolted Joints*; CRC Press: Boca Raton, FL, USA; MARCEL-DEKKER, Inc: New York, NY, USA, 1998; ISBN 0824799771.
10. Kim, J.; Lee, Y.; Yang, M. Environmental exposure to lead (Pb) and variations in its susceptibility. *J. Environ. Sci. Health-Part C Environ. Carcinog. Ecotoxicol. Rev.* **2014**, *32*, 159–185. [CrossRef]
11. Kostornov, A.G.; Fushchich, O.I.; Chevichelova, T.M.; Simeonova, Y.M.; Sotirov, G.S. Self-lubricating composite materials for dry friction. *Tribol. Ind.* **2009**, *31*, 29–32.
12. Senatore, A.; Risitano, G.; Scappaticci, L.; D'andrea, D. Investigation of the tribological properties of different textured lead bronze coatings under severe load conditions. *Lubricants* **2021**, *9*, 34. [CrossRef]
13. Wahl, K.J.; Seitzman, L.E.; Bolster, R.N.; Singer, I.L. Low-friction, high-endurance, ion-beam-deposited Pb-Mo-S coatings. *Surf. Coat. Technol.* **1995**, *73*, 152–159. [CrossRef]
14. Wahl, K.J.; Dunn, D.N.; Singer, I.L. Wear behavior of Pb-Mo-S solid lubricating coatings. *Wear* **1999**, *230*, 175–183. [CrossRef]
15. Zabinski, J.S.; Donley, M.S.; Dyhouse, V.J.; McDevitt, N.T. Chemical and tribological characterization of PbOMoS2 films grown by pulsed laser deposition. *Thin Solid Films* **1992**, *214*, 156–163. [CrossRef]
16. Zabinski, J.S.; Donley, M.S.; Walck, S.D.; Schneider, T.R.; McDevitt, N.T. The effects of dopants on the chemistry and tribology of sputter-deposited MoS2films. *Tribol. Trans.* **1995**, *38*, 894–904. [CrossRef]
17. Fleischauer, P.D.; Bauer, R. Chemical and structural effects on the lubrication properties of sputtered MoS2 films. *Tribol. Trans.* **1988**, *31*, 239–250. [CrossRef]
18. Abelson, P.H. Materials Research. *Science* **1987**, *235*, 9. [CrossRef]
19. Zabinski, J.S.; Bultman, J.E.; Sanders, J.H.; Hu, J.J. Multi-environmental lubrication performance and lubrication mechanism of MoS2/Sb2O3/C composite films. *Tribol. Lett.* **2006**, *23*, 155–163. [CrossRef]
20. Dudder, G.J.; Zhao, X.; Krick, B.; Sawyer, W.G.; Perry, S.S. Environmental Effects on the Tribology and Microstructure of MoS2–Sb2O3–C Films. *Tribol. Lett.* **2011**, *42*, 203–213. [CrossRef]
21. Everlube Products. Solid Film Lubricants. Available online: https://everlubeproducts.com/wp-content/uploads/2018/09/High-Load-Coatings (accessed on 21 December 2021).
22. Deposition Everlube Products. Available online: https://everlubeproducts.com/wp-content/uploads/2018/09/High-Load-Coatings.pdf (accessed on 21 December 2021).
23. Roy, A.; Mu, L.; Shi, Y. Tribological properties of polyimide-graphene composite coatings at elevated temperatures. *Prog. Org. Coat.* **2020**, *142*, 105602. [CrossRef]
24. Anton-Paar Force-Displacement Curve. Available online: https://wiki.anton-paar.com/en/atomic-force-microscopy-afm/ (accessed on 21 December 2021).

25. Ellis, J.S.; Allen, S.; Chim, Y.T.A.; Roberts, C.J.; Tendler, S.J.B.; Davies, M.C. Molecular-scale studies on biopolymers using atomic force microscopy. *Adv. Polym. Sci.* **2006**, *193*, 123–172. [CrossRef]
26. Bhushan, B. *An Introduction to Tribology*, 2nd ed.; John Wiley and Sons, Ltd.: New York, NY, USA, 2013; ISBN 9781119944539.
27. Singer, I.L.; Bolster, R.N.; Wegand, J.; Fayeulle, S.; Stupp, B.C. Hertzian stress contribution to low friction behavior of thin MoS 2 coatings. *Appl. Phys. Lett.* **1990**, *57*, 995–997. [CrossRef]
28. Jiang, T.; Zhu, Y. Measuring graphene adhesion using atomic force microscopy with a microsphere tip. *Nanoscale* **2015**, *7*, 10760–10766. [CrossRef]
29. Li, H.; Li, X.; Zhang, G.; Wang, L.; Wu, G. Exploring the Tribophysics and Tribochemistry of MoS2 by Sliding MoS2/Ti Composite Coating Under Different Humidity. *Tribol. Lett.* **2017**, *65*, 2–11. [CrossRef]
30. Stoyanov, P.; Chromik, R.R.; Goldbaum, D.; Lince, J.R.; Zhang, X. Microtribological Performance of Au–MoS2 and Ti–MoS2 Coatings with Varying Contact Pressure. *Tribol. Lett.* **2010**, *40*, 199–211. [CrossRef]
31. Tabor, D. Friction as Dissipative Process. *J. Frict. Wear C/C Trenie I Iznos.* **1994**, *15*, 92.
32. Hutchings, I.M. *Tribology: Friction and Wear of Engineering Materials*, 2nd ed.; Butterworth-heinemann; Elsevier Ltd.: Oxford, UK, 2017; ISBN 9780081009109.
33. Stachowiak, G.W.; Batchelor, A.W. *Engineering Tribology*, 4th ed.; Butterworth-heinemann; Elsevier Ltd.: Oxford, UK, 2014; ISBN 9780123970473.
34. Fayeulle, S.; Ehni, P.D.; Singer, I.L. Paper V (ii) Role of transfer films in wear of MoS2 coatings. *Tribol. Ser.* **1990**, *17*, 129–138. [CrossRef]
35. Godet, M. Third-bodies in tribology. *Wear* **1990**, *136*, 29–45. [CrossRef]
36. Godet, M. The third-body approach: A mechanical view of wear. *Wear* **1984**, *100*, 437–452. [CrossRef]